Ab Initio Studies on Metal−Metal Interaction and $^3[\sigma^*(d)\sigma(s)]$ Excited State of the Binuclear Au(I) Complexes Formed by Phosphine and/or Thioether Ligands

Qing-Jiang Pan and Hong-Xing Zhang*

State Key Laboratory of Theoretical and Computational Chemistry, Institute of Theoretical Chemistry, Jilin University, Changchun 130023, P. R. China

Received: January 10, 2004; In Final Form: February 20, 2004

The structures of ground state and lowest energy triplet excited state for $[Au_2(PH_2CH_2PH_2)_2]^{2+}$ (**1**), $[Au_2(PH_2CH_2PH_2)(SHCH_2SH)]^{2+}$ (**2**) and $[Au_2(SHCH_2SH)_2]^{2+}$ (**3**) as well as their solvated **1**−**3**·$(MeCN)_2$ species are fully optimized by the MP2 and CIS methods, respectively. The $^3[\sigma^*(d)\sigma(s)]$ excited states give the 300−390 emissions in the gas phase, red shifting to 500−730 nm in acetonitrile. The coordination of solvent molecule to the gold atom in the excited states is responsible for such a red shift. For **2**, all the possible geometries, the substituent effect of methyl groups on P and/or S atoms and the comparison with thiolate complex $[Au_2(PH_2CH_2PH_2)(SCH_2S)]$ (**6**) are discussed. The unrestricted MP2 calculations on **1**−**3**, head-to-tail $[Au_2(PH_2CH_2SH)_2]^{2+}$ (**7**) and head-to-head $[Au_2(PH_2CH_2SH)_2]^{2+}$ (**8**) confirm the CIS results in both optimized geometry and emissive energy related to the $^3[\sigma^*(d)\sigma(s)]$ state. The frequency calculations at the MP2 level indicate that the Au(I)−Au(I) interaction is weak in the ground state ($\nu(Au_2)$ = 89−101 cm^{-1}) but is strongly strengthened in the excited state ($\nu(Au_2)$ = 144−189 cm^{-1}).

1. Introduction

Luminescent Au(I) complexes, especially with the Au(I)−Au(I) interaction, have been receiving intense interest from different perspectives.[1−27] Extensive photoluminescence measurements have been made on this class of compounds.[1−2,4−6,12−27] The luminescent properties of bi- and polynuclear Au(I) complexes are highly diversified. In the presence of a wide range of bridging and ancillary ligands, the luminescent properties of such complexes have been suggested to range from MLCT (metal to ligand charge transfer) to LMCT (ligand to metal charge transfer) and to MC (metal-centered) transition and to ILCT (intraligand charge transfer).[19−24,28−34]

Attractive interactions between closed-shell Au(I) centers are of importance in determining the solid-state structures of many gold(I) complexes[35,36] and contribute to the properties of such complexes in solution as well.[37−40] Theoretical studies indicated that this weakly bonding interaction is the result of correlation effects that are enhanced by relativistic effects.[41−51] Experimental studies of rotational barriers showed that the strength of this attractive interaction is comparable to hydrogen bonding, ca. 7−11 kcal/mol.[37,38] Such aurophilic interactions have been shown to be strong enough to persist in solution and to play a role in guiding a chemical reaction.[39−40,52]

So far, many studies on Au(I) complexes have indicated the Au−Au aurophilicity strongly affects the luminescence.[1−2,5,29−34] Eisenberg et al. found that the binuclear dithiocarbamate complex, $[Au_2(S_2CN(C_5H_{11})_2)_2]$, crystallizes in a colorless form as well-separated dimer molecules, but forms an orange, luminescent form when exposed to the vapor of aprotic organic solvents.[2] The orange form has been crystallized from dimethyl sulfoxide and involves an extended chain of the dimers with inter- and intramolecular Au−Au separations of 2.96 and 2.77 Å. The investigations of Balch and co-workers also showed that the formation of extended chains of Au(I) centers that are connected through the Au(I)−Au(I) interactions contributes to the luminescence of Au(I) complexes.[5] Certainly, the solvent is also one of the important factors to influence the luminescence of Au(I) complexes. For example, complexes $[Au_2(dcpm)_2]X_2$ (dcpm = bis(dicyclohexylphosphino)methane, and X = Cl^-, ClO_4^-, PF_6^-, and $SO_3CF_3^-$) exhibit an intense phosphorescence at 360−368 nm in the solid state and at 490−530 nm in the acetonitrile solution.[31,32] Che et al.[31,32] have proposed that the triplet excited state of the Au(I) complexes exists as a solvent/anion exciplex in solution, whose formation results in the red shift of emission wavelength with respect to in solid state.

It has been well established that the Au−Au aurophilicity has some relationship with the excited-state properties,[53−56] especially for the binuclear Au(I) complexes that produce the lower energy emission with the MC transition property. Our previous ab initio calculations on the model complex $[Au_2(PH_2CH_2PH_2)_2]^{2+}$ (**1**) standing for real complexes $[Au_2(dmpm)_2]^{2+}$, $[Au_2(dppm)_2]^{2+}$, and $[Au_2(dcpm)_2]^{2+}$ (dmpm = bis(dimethylphosphino)methane and dppm = bis(diphenylphosphino)methane) indicated that the $^3[\sigma^*(d)\sigma(s)]$ excited state corresponding to the lower energy emission presents about 2.72 Å Au(I)−Au(I) distance, much shorter than about 3.16 Å distance in the ground state.[53] The promotion of electrons from the σ^*-(d) antibonding orbital to the σ(s) bonding orbital results in the formation of an Au−Au σ single bond in the excited state. For the famous binuclear Pt(II) complex, $[Pt_2(P_2O_5H_2)_4]^{4-}$, the Pt−Pt distance in the $^3[\sigma^*(d)\sigma(p)]$ excited state shortens about 0.29 Å relative to that in the ground state, which is supported by both the excited-state structure from time-resolved X-ray diffraction and the density functional studies.[57,58]

Binuclear gold(I) phosphine complexes, $[Au_2(diphosphine)_2]^{2+}$, have vacant coordination sites at the metal atom, feature an intense $\sigma(6s) \rightarrow \sigma^*(5d)$ transition, and have long-lived and emissive $^3[\sigma^*(d)\sigma(s)]$ excited states in fluid solutions at room temperature.[29−34] Such important excited-state properties make these complexes applied in photochemical reactions. The $[Au_2(dppm)_2]^{2+}$ complex has been reported to catalyze the photo-

10.1021/jp049873w CCC: $27.50
Published on Web 03/30/2004

chemical cleavage of C−X bonds following an electron-transfer mechanism.[33,59] The coordinatively unsaturated nature makes these Au(I) complexes suitable for the substrate-binding reaction.[32−34] With respect to abundant $[Au_2(diphosphine)_2]^{2+}$ complexes,[29−34,59−67] no systems such as $[Au_2(diphosphine)(dithioether)]^{2+}$ and $[Au_2(dithioether)_2]^{2+}$ are reported. To our best knowledge, the head-to-tail $[Au_2(PPh_2CH_2SPh)_2]\cdot(CF_3SO_3)_2$ complex[9,54,68] is one of the rare examples of the Au(I) complexes containing the thioether ligands. As the phosphine and thioether ligands both contribute lone pair electrons on P/S atoms to an Au(I) atom, forming the P/S → Au dative bond, the Au(I) complexes formed by thioether ligands are expected to have spectroscopic properties similar to those of the Au(I) phosphine complexes. Thus, the systematic theoretical studies on $[Au_2(diphosphine)_2]^{2+}$, $[Au_2(diphosphine)(dithioether)]^{2+}$, $[Au_2(phosphinothioether)_2]^{2+}$, and $[Au_2(dithioether)_2]^{2+}$, especially involved in the excited state, are necessary to provide deep insight into the photophysical and photochemical processes of the Au(I) complexes.[69]

To probe the luminescence and the attractive Au(I)−Au(I) interaction of Au(I) complexes as well as the relationship between them, the bridging ligand is introduced and the annular eight-membered binuclear Au(I) complex is an ideal candidate in both experiment[1−2,29−34,70−72] and theory.[29,43,53−56] Previous ab initio calculations indicated that correlation effect and relativistic effect should be taken into account to describe the aurophilic interaction.[41−51,53−56]

Here, we use the ab initio methods to study the Au(I)−Au(I) interaction and spectroscopic properties of a series of Au(I) complexes $[Au_2(PH_2CH_2PH_2)_2]^{2+}$ (**1**), $[Au_2(PH_2CH_2PH_2)(SHCH_2SH)]^{2+}$ (**2**), and $[Au_2(SHCH_2SH)_2]^{2+}$ (**3**) in both the gas phase and acetonitrile. The results indicate that the $^3[\sigma^*(d)\sigma(s)]$ excited states of the Au(I) complexes produce an emission in the near UV region in the gas phase whereas the emission in the acetonitrile solution red shifts to the visible region, in good agreement with the experimental observations of $[Au_2(dcpm)_2]X_2$ ($X=Cl^-$, ClO_4^-, PF_6^-, and $SO_3CF_3^-$).[31,32] The analysis from the single excitation configuration interaction (CIS)[73−75] calculations shows that the coordination of acetonitrile molecule to the gold atom on **1**−**3** for the solvated **1**·$(MeCN)_2$, **2**·$(MeCN)_2$, and **3**·$(MeCN)_2$ species is responsible for such a large red shift of emission wavelength in solution with respect to that in the gas phase. Though the CIS method only includes some electron correlation effects,[73−75] the unrestricted second-order Møller−Plesset perturbation (UMP2)[75,76] calculations on **1**−**3**, head-to-tail $[Au_2(PH_2CH_2SH)_2]^{2+}$ (**7**) and head-to-head $[Au_2(PH_2CH_2SH)_2]^{2+}$ (**8**) prove that the results from the CIS calculations are reasonable.

2. Computational Details and Theory

In the calculations, we use $[Au_2(PH_2CH_2PH_2)_2]^{2+}$ (**1**), $[Au_2(PH_2CH_2PH_2)(SHCH_2SH)]^{2+}$ (**2**), and $[Au_2(SHCH_2SH)_2]^{2+}$ (**3**) as the computational models to represent a series of eight-membered ring Au(I) complexes with bridging phosphine and/or thioether ligands. The similar model was applied in many works by using hydrogen to replace methyl, phenyl, cyclohexyl, etc. heavy substituents in ab initio studies to save the computational resources.[3,29,53−56,77−79] Rösch et al.[80,81] have proved that PH_3 provides a satisfactory model of the full PPh_3 or PMe_3 for structural properties of Au(I) complexes. The models $[Au_2(PH_2CH_2PH_2)(SCH_3CH_2SCH_3)]^{2+}$ (**4**) and $[Au_2(P(CH_3)_2CH_2P(CH_3)_2)(SCH_3CH_2SCH_3)]^{2+}$ (**5**) are calculated to reveal the substituent effect of methyl groups on sulfur and/or phosphor atoms on geometry structures, electronic structures, and spectroscopic properties of Au(I) complexes.

The calculations on the single Au(I) molecule correspond to the properties of the molecule in the gas phase.[75,82] The weakly solvated $[Au_2(PH_2CH_2PH_2)_2]^{2+}\cdot(MeCN)_2$ (**1**·$(MeCN)_2$), $[Au_2(PH_2CH_2PH_2)(SHCH_2SH)]^{2+}\cdot(MeCN)_2$ (**2**·$(MeCN)_2$), $[Au_2(SHCH_2SH)_2]^{2+}\cdot(MeCN)_2$ (**3**·$(MeCN)_2$), $[Au_2(PH_2CH_2PH_2)(SCH_3CH_2SCH_3)]^{2+}\cdot(MeCN)_2$ (**4**·$(MeCN)_2$), and $[Au_2(P(CH_3)_2CH_2P(CH_3)_2)(SCH_3CH_2SCH_3)]^{2+}\cdot(MeCN)_2$ (**5**·$(MeCN)_2$) species are employed to simulate the behaviors of **1**−**5** in the acetonitrile solution. In our previous investigations,[53,54] the supramolecular model of the acetonitrile solvation has successfully explained and predicted luminescent properties of Au(I) complexes in solution.

In this work, **2** takes the boat conformation with the C_s symmetry, and **1** and **3** chose the chair ones with the C_i symmetry when additional calculations on their solvated species are considered. We also fully optimize various possible geometries of **2** and **2**·$(MeCN)_2$ using the MP2 method for the ground state and the CIS method for the excited state (Supporting Information). The detailed results are not reported here.

It is well-known that CIS represents a general zeroth-order method for excited states and belongs to a state-based electronic theory for excited-state chemistry, just as HF is for the ground state of molecular systems.[73−75,82] Besides being relatively inexpensive, permitting it to be applied to large molecules such as **4**·$(MeCN)_2$ and **5**·$(MeCN)_2$, the wave function, energy, and analytic gradient of a molecule in an electronically excited state are available for the CIS method.[73−75,82] However, as CIS uses the orbitals of a HF state in an ordinary CI procedure to solve for the higher roots and only includes some of the electron correlation effects via the mixing of excited determinants, the transition energy from the CIS calculations are usually overestimated.[73,82−84] To certify the validity of the CIS method for the Au(I) complexes in the paper, the unrestricted MP2 method is employed to calculate the lowest energy triplet excited states of **1**−**3**, head-to-tail $[Au_2(PH_2CH_2SH)_2]^{2+}$ (**7**), and head-to-head $[Au_2(PH_2CH_2SH)_2]^{2+}$ (**8**). The subsequent frequency calculations at the MP2 level confirm the optimized ground- and excited-state geometries are all minima because of no imaginary frequency available.

In the calculations, quasi-relativistic pseudopotentials of the Au, S, and P atoms proposed by Hay and Wadt[85,86] with 19, 6, and 5 valence electrons, respectively, are employed and the LanL2DZ basis sets associated with the pseudopotential are adopted. One additional f-type function is implemented for Au ($\alpha_f = 0.2$) and one d-type function is added to S ($\alpha_d = 0.421$) and to P ($\alpha_d = 0.34$), respectively.[41−51,54−56] In the previous study on **1**,[53] the Au and P atoms are not augmented by the f and d polarization functions. It has been found that such polarization functions are required for precisely describing the aurophilic interaction[41−43] and the potential energy surface of excited states.[73] In Table 1, the comparison between with and without d- and f-type polarization functions in the optimized ground-state geometries for **1** and **7** indicates that the introduction of polarization functions makes the results closer to the experimental values.[32,68] Here, the basis sets are taken as Au(8s6p3d1f/3s3p2d1f), S(3s3p1d/2s2p1d), P(3s3p1d/2s2p1d), N(10s5p/3s2p), C(10s5p/3s2p), and H(4s/2s). Thus, 152 basis functions and 80 electrons for **1**, 218 basis functions and 124 electrons for **1**·$(MeCN)_2$, 148 basis functions and 80 electrons for **2**, 214 basis functions and 124 electrons for **2**·$(MeCN)_2$, 144 basis functions and 80 electrons for **3**, 210 basis functions and 124 electrons for **3**·$(MeCN)_2$, 174 basis functions and 96 electrons for **4**, 240 basis functions and 140 electrons for **4**·$(MeCN)_2$, and 226 basis functions and 128 electrons for **5**, and

TABLE 1: Optimized Geometry Parameters in the Ground States of $[Au_2(PH_2CH_2PH_2)_2]^{2+}$ (1) and Head-to-Tail $[Au_2(PH_2CH_2SH)_2]^{2+}$ (7) Using the MP2 Method, Associated with the Data from X-ray Crystal Diffraction[a]

	1			7		
basis sets	I[b]	II[c]	exp[d]	I[b]	II[c]	exp[e]
Au−Au	3.165	3.033	2.939	3.081	2.979	2.902
Au−P	2.451	2.377	2.318	2.427	2.341	2.272
Au−S				2.514	2.424	2.362
P···P/S	3.194	3.104		3.244	3.160	
P−Au−P/S	179.3	178.3	173.9	175.5	174.9	175.1
P−Au−Au	90.3	90.8	92.2	88.9	87.1	91.4
S−Au−Au				94.7	97.0	93.5

[a] Distances in angstroms, and bond angles in degrees. [b] Basis set I: LanL2DZ. [c] Basis set II: LanL2DZ augmented by one d-type and one f-type polarization functions for P and Au atoms, respectively. [d] The experimental values of $[Au_2(dcpm)_2]\cdot(ClO_4)_2$ from ref 32. [e] The experimental values of $[Au_2(PPh_2CH_2SPh)_2]\cdot(CF_3SO_3)_2$ from ref 68.

292 basis functions and 172 electrons for $\mathbf{5}\cdot(MeCN)_2$ are included in the calculations. All the calculations are accomplished by using the *Gaussian98* program package[75] on an Origin/3800 server.

3. Results and Discussion

In recent years, extensive studies have been performed on the photoluminescence and photophysical properties of binuclear gold(I) phosphine complexes.[29−34] The lowest energy phosphorescent emission of such complexes was assigned as a metal-centered transition by theoretical[29,53] and experimental studies.[29−34] The structural characterization from the X-ray crystal diffraction[32,61−66] indicated that the crystalline forms a series of discrete binuclear Au(I) dimers; i.e., there are no intermolecular Au(I)−Au(I) interactions. In each discrete dimer, the cations such as $[Au_2(dmpm)_2]^{2+}$, $[Au_2(dppm)_2]^{2+}$, and $[Au_2(dcpm)_2]^{2+}$ weakly interact with counteranions such as ClO_4^-, PF_6^-, Cl^-, Br^-, and I^-. Such a crystal structure of the binuclear Au(I) phosphine complex shows that the lower energy emission is mainly correlated with intramolecular Au(I)−Au(I) interactions and the counteranions have a small effect on the emission.[53,54] Therefore, this type of complexes is suitable for the theoretical studies, and can be modeled by $[Au_2(PH_2CH_2PH_2)_2]^{2+}$, $[Au_2(PH_2CH_2PH_2)_2]^{2+}\cdot(X)_2$ (X = counteranion), and $[Au_2(PH_2CH_2PH_2)_2]^{2+}\cdot(MeCN)_2$, corresponding to the behaviors of the gas phase, solid state, and solution, respectively.

It is important to study the factors affecting the photophysical and photochemical properties of luminescent gold(I) complexes, which have been receiving growing interest over the past several years.[32−34,87] The open coordination framework of two-coordinate gold(I) is important for it to be able to undergo substrate-binding reactions in the ground and excited states.[29−34] The studies[32] on the association constants of $[Au_2(dcpm)_2]^{2+}$ and halide ions indicated that the high affinity of two-coordinate gold(I) to undergo substrate-binding reactions is in contrast to the square-planar d^8 platinum(II) system, which remains four-coordinate in most instances.[88,89] It is of interest to compare the binuclear Au(I) phosphine with the classic binuclear platinum(II) photocatalyst $[Pt_2(P_2O_5H_2)_4]^{4-}$ in both experiment and theory.[90−98]

3.1. Ground- and Excited-State Structures of 1−3 and Their Solvated Species. The full MP2 optimizations on the ground states of **1**−**3** are performed for the chair, boat, and chair conformations with the C_i, C_s, and C_i symmetries, respectively. Accordingly, the three Au(I) complexes have the ^1A_g, $^1A'$, and ^1A_g ground electronic states. The optimized main geometry parameters and structures are presented in Table 2 and Figure 1a−c. The calculated results indicate that the Au(I) and P/S atoms for **1**−**3** are nearly coplanar because of the P/S−Au−Au−P/S dihedral angles of +180.0°, −178.7°, and +180.0°. The Au(I) atom takes the typical linear two-coordinated geometry[1−4,15−24] with the largest deviation of 7.0° from 180° for the S−Au−S angle of **3**. The calculated Au(I)−Au(I) distances for **1**−**3** are 3.033, 2.989, and 2.944 Å, much less than the van der Waals contact of 3.4 Å.[99] Moreover, the Au−Au distances are about 0.1−0.2 Å shorter than the corresponding P/S···P/S bite distances, as seen in Table 2. Thus, the two Au(I) atoms in **1**−**3** tend to approach each other, showing the weak Au−Au aurophilic interaction. In addition, the Au−S bond length is apparently longer than the Au−P one, about 0.1 Å. This implies the coordination ability to the Au(I) atom decreases from P to S; i.e., PH_3 is a stronger base than SH_2. This is also

TABLE 2: Optimized Geometry Parameters of $[Au_2(PH_2CH_2PH_2)_2]^{2+}$ (1), $[Au_2(PH_2CH_2PH_2)(SHCH_2SH)]^{2+}$ (2), $[Au_2(SHCH_2SH)_2]^{2+}$ (3), $[Au_2(PH_2CH_2PH_2)(SCH_3CH_2SCH_3)]^{2+}$ (4), and $[Au_2(P(CH_3)_2CH_2P(CH_3)_2)(SCH_3CH_2SCH_3)]^{2+}$ (5) Using the MP2 Method for the Ground State and the CIS Method for the Excited State

	1		2		3		4		5	
parameters[a]	^1A_g	^3A_u	$^1A'$	$^3A''$	^1A_g	^3A_u	$^1A'$	$^3A''$	$^1A'$	$^3A''$
Au−Au	3.033	2.750	2.989	2.708	2.944	2.694	2.985	2.710	2.960	2.693
Au−P	2.377	2.516	2.343	2.545			2.344	2.547	2.329	2.492
Au−S			2.422	2.711	2.390	2.669	2.400	2.626	2.411	2.681
P−C	1.874	1.861	1.873	1.863			1.873	1.864	1.869	1.866
P−C′									1.853	1.840
P−C″									1.852	1.842
S−C			1.860	1.837	1.860	1.838	1.856	1.836	1.855	1.837
S−C′							1.864	1.834	1.862	1.833
P···P	3.104	3.136	3.107	3.139			3.100	3.147	3.172	3.229
S···S			3.237	3.187	3.236	3.184	3.274	3.224	3.267	3.233
P···S										
P−Au−S			175.4	170.1			174.9	169.0	173.6	166.8
P−Au−P	178.3	171.2								
S−Au−S					173.0	169.4				
P−Au−Au	90.9	94.4	91.4	94.9			91.4	94.9	92.6	96.2
S−Au−Au			92.9	95.1	93.5	95.3	93.5	95.6	93.6	95.8
C′S−Au							105.7	110.2	105.6	110.6
C′P−Au									113.8	113.5
C″−Au									113.7	119.4
P/S−Au−Au−P/S	180.0	179.9	−178.7	179.8	180.0	180.0	178.5	−176.9	178.4	174.4

[a] Distances in angstroms, and bond angles and dihedral angles in degrees.

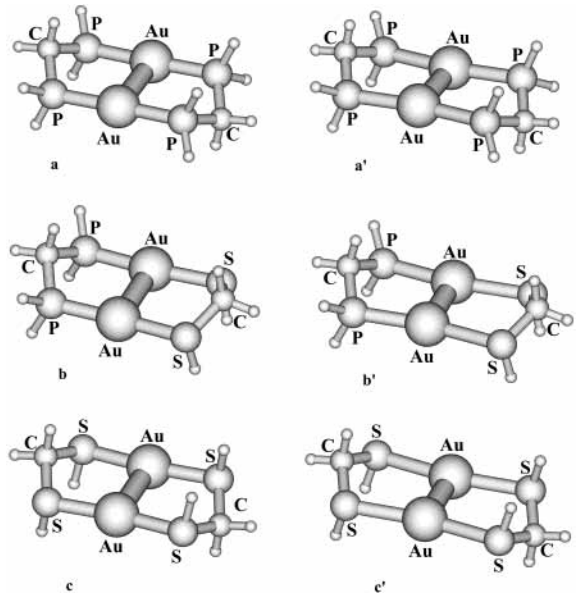

Figure 1. Ground-state (a)−(c) and excited-state (a′)−(c′) structures of $[Au_2(PH_2CH_2PH_2)_2]^{2+}$ (**1**), $[Au_2(PH_2CH_2PH_2)(SHCH_2SH)]^{2+}$ (**2**), and $[Au_2(SHCH_2SH)_2]^{2+}$ (**3**) optimized by the MP2 and CIS methods, respectively.

reflected in **2**, where the Au−P distance shortens 0.03 Å and the Au−S distance elongates 0.03 Å with respect to corresponding ones in **1** and **3**.

For the excited states of **1**−**3**, the CIS method is applied to fully optimize their structures, corresponding to ^3A_u, $^3A''$, and ^3A_u states. The calculated main geometry parameters and structures are presented in Table 2 and Figure 1a′−c′, respectively. Corresponding to their ground states, the Au(I)−Au(I) interaction is strongly enhanced, which weakens the interactions between the Au and P/S atoms. The Au(I)−Au(I) bond lengths of **1**−**3** are 2.750, 2.708, and 2.694 Å, comparable to the Au−Au σ single bond in some binuclear Au(II) complexes.[100,101] Recently, Pyykkö et al. have calculated the geometric and electronic structures of the $^3\Sigma_u^+$ excited state for the Au_2^{2+} species using the higher level CASPT2 method.[102] The calculated Au(I)−Au(I) distance of 2.51 Å can be served as a lower limit. Our calculated Au(I)−Au(I) distances abide by such a limit.

The weakly solvated **1**·$(MeCN)_2$, **2**·$(MeCN)_2$, and **3**·$(MeCN)_2$ species are used to account for the solvent effect of acetonitrile. According to the previous studies,[53,54] the supramolecular model is reasonable to explain the properties of the Au(I) complex in the acetonitrile solution for the ground and excited states. We listed in Table 3 and Figure 2 the optimized geometry parameters and structures for the solvated species. In the ground state, the Au−N distance is about 2.57 Å in **1**−**3**·$(MeCN)_2$ and the weak interaction between Au(I) of cation and N of acetonitrile results in the about 13° deviation of P/S−Au−Au−P/S dihedral angles from the original about 180° ones of **1**−**3**; the Au(I)−Au(I), Au−P/S, and P/S···P/S distances are nearly unchanged in acetonitrile with respect to in gas phase. For the **1**·$(MeCN)_2$, **2**·$(MeCN)_2$, and **3**·$(MeCN)_2$ species, the geometry structures of the excited states have the following two major changes compared with those of the corresponding ground states, as seen in Table 3. First, the N−Au−Au angle changes from 100−135° in the ground states to 173−180° in the excited states, namely, the Au atoms, P/S atoms, and acetonitrile molecules lie upon a plane. The interaction between the Au(I) and N atoms is greatly enhanced, for the Au−N distances of the excited states are about 0.22 Å shorter than those of the ground states. Second, the Au(I)−Au(I) separations are greatly shortened from about 2.97 Å (mean value) to about 2.65 Å upon excitation. However, the distances of Au−P/S are strongly elongated, caused by the Au(I)−Au(I) bonding interaction weakening the S → Au and P → Au bonds just like the case in gas phase on one hand and the competition among the N → Au, S → Au, and P → Au coordination on the other hand. Because the weakening of Au−P/S bonds arising from the enhancement of the Au(I)−Au(I) bonding in the excited state exists in both the gas phase and acetonitrile, we may simply consider the difference between the gas phase and acetonitrile in the Au−P/S distances of the excited states is the result of the competition of N → Au and

TABLE 3: Optimized Geometry Parameters of $[Au_2(PH_2CH_2PH_2)_2]^{2+}$·$(MeCN)_2$ (1·$(MeCN)_2$), $[Au_2(PH_2CH_2PH_2)(SHCH_2SH)]^{2+}$·$(MeCN)_2$ (2·$(MeCN)_2$), $[Au_2(SHCH_2SH)_2]^{2+}$·$(MeCN)_2$ (3·$(MeCN)_2$), $[Au_2(PH_2CH_2PH_2)(SCH_3CH_2SCH_3)]^{2+}$·$(MeCN)_2$ (4·$(MeCN)_2$), and $[Au_2(P(CH_3)_2CH_2P(CH_3)_2)(SCH_3CH_2SCH_3)]^{2+}$·$(MeCN)_2$ (5·$(MeCN)_2$) Using the MP2 Method for the Ground State and the CIS Method for the Excited State

	1·$(MeCN)_2$		**2**·$(MeCN)_2$		**3**·$(MeCN)_2$		**4**·$(MeCN)_2$		**5**·$(MeCN)_2$	
parameters[a]	^1A_g	^3A_u	$^1A'$	$^3A''$	^1A_g	^3A_u	$^1A'$	$^3A''$	$^1A'$	$^3A''$
Au−Au	2.997	2.720	3.047	2.655	2.925	2.620	3.053	2.671	3.017	2.658
Au−P	2.366	2.688	2.327	2.596			2.332	2.635	2.317	2.529
Au−S			2.442	3.030	2.394	2.800	2.413	2.820	2.416	2.971
P−C	1.873	1.859	1.869	1.858			1.869	1.859	1.866	1.857
P−C′									1.854	1.841
P−C″									1.854	1.843
S−C			1.852	1.830	1.856	1.830	1.849	1.828	1.850	1.827
S−C′							1.861	1.831	1.859	1.828
Au−N	2.600	2.427	2.584	2.336	2.522	2.309	2.673	2.380	2.774	2.405
P···P	3.077	3.074	3.071	3.066			3.071	3.073	3.151	3.153
S···S			3.185	3.127	3.196	3.137	3.244	3.172	3.247	3.167
P−Au−S			168.0	170.9			174.5	169.8	174.6	153.8
P−Au−P	168.1	172.5								
S−Au−S					164.1	169.4				
P−Au−Au	90.7	93.8	90.3	94.5			90.2	94.4	91.7	95.6
S−Au−Au			91.6	94.5	91.5	95.3	92.3	95.1	92.7	94.9
C′S−Au							104.4	107.3	104.1	107.9
C′P−Au									113.9	112.0
C″P−Au									113.9	118.8
N−Au−Au	99.5	180.0	134.5	173.2	114.4	180.0	160.3	175.8	161.0	167.7
P/S−Au−Au−S/P	168.1	180.0	168.2	179.0	164.9	180.0	175.1	176.3	176.8	156.0

[a] Distances in angstroms, and bond angles and dihedral angles in degrees.

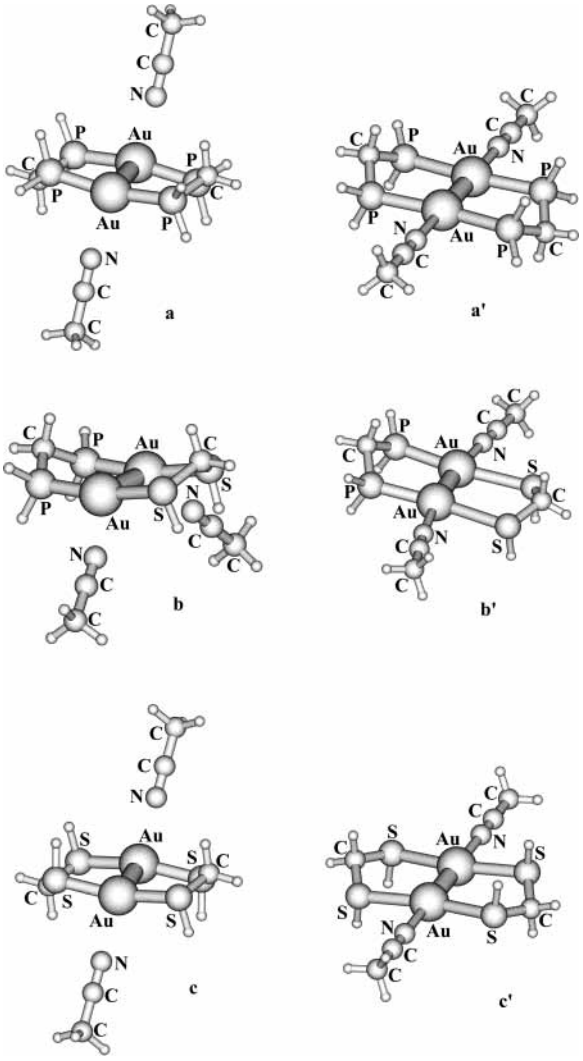

Figure 2. Ground-state (a)−(c) and excited-state (a′)−(c′) structures of $[Au_2(PH_2CH_2PH_2)_2]^{2+}\cdot(MeCN)_2$ (**1**·$(MeCN)_2$), $[Au_2(PH_2CH_2PH_2)(SHCH_2SH)]^{2+}\cdot(MeCN)_2$ (**2**·$(MeCN)_2$), and $[Au_2(SHCH_2SH)_2]^{2+}\cdot(MeCN)_2$ (**3**·$(MeCN)_2$) under the MP2 and CIS calculations, respectively.

S/P → Au. The N → Au coordination leads to 0.27 Å Au−P and 0.10 Å Au−S longer for the pure phosphine **1**·$(MeCN)_2$ and thioether **3**·$(MeCN)_2$ complexes, respectively, and to 0.04 Å Au−P and 0.31 Å Au−S longer for the phosphine thioether complex, **2**·$(MeCN)_2$. Apparently, the case among the N → Au, S → Au, and P → Au coordination is more complicated in **2**·$(MeCN)_2$ due to the inclusion of the competition between the S → Au and P → Au coordination.

For the coordinatively unsaturated **1**−**3**, the adducts form between cations and acetonitrile molecules in the excited states of **1**−**3**·$(MeCN)_2$. Our calculated results confirm the proposal of Che et al.[31,32] that the triplet excited state of the $[Au_2(dcpm)_2]X_2$ (X = Cl^-, ClO_4^-, PF_6^-, and $SO_3CF_3^-$) complexes exists as a solvent exciplex in solution. In fact, many geometries similar to **1**−**3**·$(MeCN)_2$ in the excited states have been synthesized and structurally characterized, such as binuclear d^9 Au(II) complexes.[100−101,103−105] So the lowest energy emissions of **1**−**3** and their solvated species are expected to correlate with *n*d → (*n*+1)s/p transitions.

3.2. Luminescent Properties of 1−3 and Their Solvated Species. So far, the luminescence of many binuclear Au(I) phosphine complexes such as $[Au_2(dppm)_2]^{2+}$ and $[Au_2(dcpm)_2]^{2+}$ has been reported.[29−34] At room temperature,

TABLE 4: Natural Atomic Orbital Populations of the Lowest Energy Triplet Excited State and the Corresponding Ground State for $[Au_2(PH_2CH_2PH_2)_2]^{2+}$ (1), $[Au_2(PH_2CH_2PH_2)(SHCH_2SH)]^{2+}$ (2), and $[Au_2(SHCH_2SH)_2]^{2+}$ (3) under the CIS Calculations

		1		2		3	
atom	orbital	^1A_g	^3A_u	$^1A'$	$^3A''$	^1A_g	^3A_u
Au	6s	0.712	0.742	0.602	0.776	0.498	0.756
	6p	0.012	0.144	0.016	0.076	0.020	0.054
	5d	9.856	9.623	9.875	9.631	9.891	9.635
	4f	0.003	0.005	0.003	0.004	0.003	0.004
P	3s	1.334	1.338	1.333	1.340		
	3p	3.150	3.159	3.149	3.127		
	3d	0.056	0.055	0.057	0.056		
S	3s			1.661	1.664	1.662	1.665
	3p			4.233	4.228	4.224	4.195
	3d			0.039	0.039	0.041	0.040
C	2s	1.220	1.232	1.221	1.229	1.190	1.194
	2p	3.782	3.784	3.782	3.782	3.442	3.444

$[Au_2(dppm)_2]^{2+}$ [29,33−34] and $[Au_2(dcpm)_2]^{2+}$ [31,32] exhibit the intense phosphorescent emissions at 565−593 and 490−530 nm in acetonitrile, respectively, and the latter displays the emissions at 360−368 nm in the solid state. The dppm ligand possesses not only the steric effect like the dcpm ligand but also the electronic effect from phenyl group on P atoms. The difference of the two types of Au(I) complexes in fluid emission wavelength mainly results from such a reason. In addition, the dcpm intraligand transition occurs at a much higher energy than the σ^*(5d) → σ(6s) transition, whereas the π → π^* transition of phenyl rings of the dppm ligand is close in energy to the σ^*(5d) → σ(6s) transition, leading to no intense high-energy emission available for $[Au_2(dppm)_2]^{2+}$ in the solid state at room temperature.[31,32] In fact, our model $[Au_2(PH_2CH_2PH_2)_2]^{2+}$ can stand for the real $[Au_2(dmpm)_2]^{2+}$, $[Au_2(dppm)_2]^{2+}$, and $[Au_2(dcpm)_2]^{2+}$ complexes and reflect the emissive transition in nature just because the lower energy emissions of such Au(I) complexes mainly originate from the σ^*(5d) → σ(6s) transitions and are strongly correlated with the Au(I)−Au(I) interaction.

In the CIS calculations, **1**−**3** give the lowest energy phosphorescent emissions at 301, 346, and 387 nm in the gas phase and at 507, 677, and 727 nm in acetonitrile solution, respectively. To conveniently discuss the emissive process, we present the natural atomic orbital populations of the triplet excited state and the corresponding ground state in Tables 4 and 5.

In the previous theoretical investigations,[58,105−109] Mulliken populations were used to present the information concerning atomic charge distributions to render a chemical interpretation of the wave function, and to get a useful understanding and correlation of chemical phenomena. Though, of the numerous schemes proposed for atomic population analysis, only that of Mulliken has truly found widespread use, unfortunately, as has been repeatedly mentioned in the literature, Mulliken populations fail to give a useful and reliable characterization of the charge distribution in many cases.[110−112] Because Mulliken populations seem to give an unreasonable physical picture of the charge distribution in compounds having significant ionic character and are unduly sensitive to basis set, particularly as the basis set is enlarged to higher accuracy, here the natural population analysis proposed by Löwdin[113] is applied to solve the problems about atomic charges and orbital populations of molecular wave functions. The natural analysis is an alternative to conventional Mulliken population analysis and can exhibit improved numerical stability and better describe the electron distribution in compounds of high ionic character, such as those containing metal atoms.[110]

TABLE 5: Natural Atomic Orbital Populations of the Lowest Energy Triplet Excited State and the Corresponding Ground State for $[Au_2(PH_2CH_2PH_2)_2]^{2+}\cdot(MeCN)_2$ ($1\cdot(MeCN)_2$), $[Au_2(PH_2CH_2PH_2)(SHCH_2SH)]^{2+}\cdot(MeCN)_2$ ($2\cdot(MeCN)_2$), and $[Au_2(SHCH_2SH)_2]^{2+}\cdot(MeCN)_2$ ($3\cdot(MeCN)_2$) under the CIS Calculations

		$1\cdot(MeCN)_2$		$2\cdot(MeCN)_2$		$3\cdot(MeCN)_2$	
atom	orbital	^1A_g	^3A_u	$^1A'$	$^3A''$	^1A_g	^3A_u
Au	6s	0.542	0.783	0.457	0.763	0.402	0.744
	6p	0.015	0.038	0.017	0.036	0.019	0.035
	5d	9.888	9.632	9.896	9.618	9.906	9.603
	4f	0.002	0.003	0.002	0.003	0.003	0.003
P	3s	1.364	1.370	1.354	1.351		
	3p	3.143	3.128	3.151	3.104		
	3d	0.050	0.050	0.052	0.052		
S	3s			1.668	1.669	1.667	1.667
	3p			4.267	4.273	4.243	4.223
	3d			0.034	0.034	0.036	0.036
C	2s	1.217	1.221	1.216	1.222	1.185	1.187
	2p	3.781	3.780	3.788	3.783	3.452	3.451
N	2s	1.573	1.561	1.563	1.552	1.558	1.548
	2p	4.029	4.024	4.069	4.060	4.089	4.078
C_N	2s	0.885	0.884	0.888	0.887	0.889	0.888
	2p	2.603	2.604	2.569	2.570	2.554	2.555
C_H	2s	1.134	1.134	1.124	1.124	1.125	1.125
	2p	3.555	3.555	3.552	3.552	3.552	3.552

It can be seen from Tables 4 and 5 that the charge transfer localized on gold centers plays a main role in the transitions. For the emissive process, the electrons mainly transfer from 6s to 5d orbitals of the Au(I) atom, belonging to the metal-centered transition, whereas the populations on other atoms are nearly unchanged. For **2**, the electronic configuration of Au atom is $4f^{0.003}5d^{9.875}6s^{0.602}6p^{0.016}$ and $4f^{0.004}5d^{9.631}6s^{0.776}6p^{0.076}$ for the $^1A'$ ground state and the $^3A''$ excited state, respectively. The 5d orbital gets a total of about 0.24 e from 6s (0.17 e) and 6p (0.06 e) orbitals. In addition, about 0.01−0.02 e of the 2p orbitals of S/P atoms is back-donated from Au atoms in the 346 nm $^3A'' \rightarrow {}^1A'$ transition. Because the interaction between the two Au(I) atoms combines the 5d orbitals and the 6s orbitals into the σ^*(d) (HOMO) and σ(s) (LUMO) orbitals, respectively, the 346 nm phosphorescence is assigned as a $\sigma(6s) \rightarrow \sigma^*(5d)$ transition from the excited state to the ground state. Accordingly, the $^3[\sigma^*(d)\sigma(s)]$ excited state presents a much shorter Au(I)−Au(I) distance of 2.708 Å compared with 2.989 Å in the ground state for **2**, as shown in Table 2. For **1**−**3**, the emissions change from 301 to 346 to 387 nm with the variation of the $PH_2CH_2PH_2$ (phosphine) and $SHCH_2SH$ (thioether) ligands, parallel with the increase of charge transfer in the $\sigma(s) \rightarrow \sigma^*(d)$ transitions (Table 4) and the decrease of Au(I)−Au(I) distance in the $^3[\sigma^*(d)\sigma(s)]$ excited states (Table 2) upon going from **1** to **3**. The greater 6s contribution to the transition should result in the lower emissive energy (longer emission wavelength) and the larger relativistic contraction (shorter Au(I)−Au(I) distance). Thus, we can simply correlate the Au(I)−Au(I) distance with the emission wavelength; i.e., the shorter the Au(I)−Au(I) distance, the longer the emission wavelength. It is, indeed, the case for **1**−**3**$\cdot(MeCN)_2$ because of 2.720, 2.655, and 2.620 Å Au(I)−Au(I) distances in the excited states and 507, 677, and 727 nm emissions. Thus, the interchange of the $PH_2CH_2PH_2$ (phosphine) and $SHCH_2SH$ (thioether) ligands makes the regular variation of Au(I)−Au(I) distance and emission wavelength in **1**−**3** complexes.

In the $^3[\sigma^*(d)\sigma(s)]$ excited states of **1**−**3** in the acetonitrile solution, the adducts form between **1**−**3** cations and acetonitrile molecules as Che et al. suggested. The **1**−**3**$\cdot(MeCN)_2$ complexes in the excited states resemble the binuclear Au(II) complexes in the geometry structure.[100−101,103−104] It is the coordination from N to Au(I) that strongly increases the charge transfer between the σ^*(d) and σ(s) orbitals, resulting in a longer emission wavelength and a shorter Au(I)−Au(I) distance in **1**−**3**$\cdot(MeCN)_2$ with respect to those in **1**−**3**, as seen in Tables 2−5. Namely, the 6s orbitals of Au(I) atoms lose about 0.24, 0.31, and 0.34 e in solution and about 0.03, 0.17, and 0.26 e in the gas phase for **1**−**3**, respectively. In the emissive processes of **1**−**3**$\cdot(MeCN)_2$, 2s and 2p orbitals of N atoms both contribute about 0.01 e, indicating the use of the (sp) electrons of N to coordinate to Au(I).

To deeply understand the electronic structures of **1**−**3**$\cdot(MeCN)_2$ in the excited states, we list their partial frontier molecular compositions in the $^3[\sigma^*(d)\sigma(s)]$ excited states in Table 6 and Tables 1 and 2 of the Supporting Information. Most

TABLE 6: Partial Molecular Orbital Contributions (%) of the Lowest Energy ^3A_u Excited State of $[Au_2(PH_2CH_2PH_2)_2]^{2+}\cdot(MeCN)_2$ ($1\cdot(MeCN)_2$) under the CIS Calculations

			contribution (%)			Au components			others components		
orbital	bond	energy (eV)	2Au	4P	2N	s	p	d			
$35a_u$	$\pi + \sigma(P_2)$	−1.937	32	36	0		28% p_y		8% p_y(P)	7% p_z(P)	
$35a_g$	π^*	−2.256	88	10	0		87% p_x				
$34a_g$	σ	−2.468	66	9	0	18% s	48% p_z				
$34a_u$	π	−2.942	47	31	0		47% p_x		9% s(P)	5% p_z(P)	
$33a_g$	π^*	−3.014	89	3	0		86% p_y				
$33a_u$	σ^*	−3.016	62	11	2	6% s	56% p_z		6% s(P)		
$32a_u$	π	−4.565	54	9	0		52% p_y				
$32a_g$	σ	−5.316	43	43	2	23% s	11% p_z	5% d_{y2}	11% s(P)	9% p_x(P)	
						HOMO−LUMO Gap					
$31a_u$	σ^*	−14.332	56	29	9			40% d_{x2-z2} 13% d_{y2}	5% s(P)	9% p_x(P)	6% s(N)
$30a_u$	σ(Au−P)	−16.714	13	57	2		13% p_x		24% p_x(P)		
$31a_g$	σ(Au−P)	−16.784	33	57	1		10% p_x	22% d_{xz}	6% s(P)	22% p_x(P)	
$30a_g$	σ	−16.912	54	23	8	16% s	5% p_z	31% d_{y1}	9% p_x(P)		
$29a_g$	$\pi^* + \pi$(C≡N)	−17.878	82	0	9			82% d_{yz}	9% p_y(N)		
$29a_u$	σ^*	−18.031	95	2	2			46% $d_{x^1-z^2}$ 43% d_{y2}			
$28a_g$	$\pi^* + \pi$(C≡N)	−18.049	67	3	14			66% d_{xz}	14% p_x(N)		
$28a_u$	$\pi + \pi$(C≡N)	−18.517	21	0	39			21% d_{yz}	39% p_y(N)		
$27a_u$	$\pi + \pi$(C≡N)	−18.602	21	1	38			21% d_{xz}	38% p_x(N)		
$26a_u$	δ^*	−18.743	97	1	0			97% d_{xy}			
$27a_g$	δ	−18.906	91	3	1			86% d_{xy}			
$26a_g$	$\pi^* + \pi$(C≡N)	−18.934	32	0	34			31% d_{yz}	34% p_y(N)		
$25a_g$	$\pi^* + \pi$(C≡N)	−18.990	25	14	25			24% d_{xz}	24% p_x(N)		
$24a_g$	σ	−19.055	82	1	12			42% $d_{x^2-z^2}$ 30% d_{y^2}	7% s(N)	5% p_z(N)	

of the orbitals can be assigned as a single-bonding function from the combination of gold(I) atomic orbitals. In the three excited-state geometries, the *z* axis goes through two Au(I) atoms. The Au and P atoms lie upon the *xz* plane for **1**·$(MeCN)_2$, whereas the Au and P/S atoms lie on the *yz* plane for **2**−**3**·$(MeCN)_2$.

With respect to **1**·$(MeCN)_2$ in the triplet excited state, the occupied orbitals have the most Au 5d characters, associated with some participation of the phosphor on phosphine ligand and of the C≡N bonding on acetonitrile, whereas the unfilled orbitals possess the most Au 6s and 6p characters, as seen in Table 6. The $30a_u$ and $31a_g$ molecular orbitals (MOs) have the metal−ligand σ bonding characters, where the former is combined by 13% p_x(Au) and 24% p_x(P) and the latter mainly arises from the interplay between the p_x(P) atomic orbital and the admixture of the p_x(Au) and d_{xz}(Au) atomic orbitals (AOs). It is seen that the interactions of the d_{xy}(Au) AOs form the δ and δ* bonds in $27a_g$ and $26a_u$ MOs, respectively, with about 0.16 eV separated energy. The π orbitals come from the d_{xz}-(Au) and d_{yz}(Au) AOs, where the d_{xz} π ($27a_u$) and π* ($28a_g$) orbitals are separated by about 0.55 eV and the d_{yz} π ($28a_u$) and π* ($29a_g$) orbitals are separated by about 0.64 eV. Apparently, dπ interactions are more significant than dδ. It is worth noting that there is some π(C≡N) bonding contribution to each π MO of metal. Moreover, the π(C≡N) bonding characters are greater in lower energy metal π MOs than in higher energy metal π MOs, showing the binding of acetonitrile to Au(I) atom can stabilize the $^3[\sigma^*(d)\sigma(s)]$ excited state of **1**·$(MeCN)_2$. For the four metal−metal σ and σ* orbitals: the $31a_u$ (HOMO) and $29a_u$ are the metal−metal σ* MOs, mainly contributed by the combination of $d_{x^2-z^2}$(Au) and d_{y^2}(Au) AOs; the $30a_g$ σ bonding orbital is mixed by 31% d_{y^2}(Au), 16% s(Au), and 5% p_z(Au) AOs; the $24a_g$ is a σ bonding orbital with the mixed 42% $d_{x^2-z^2}$(Au) and 30% d_{y^2}(Au) orbital characters. Except for the most Au 5d components in $31a_u$ and $24a_g$ orbitals, about 10% s(N) + p_z(N) character is found, suggesting the sp hybrid electrons of acetonitrile are used to coordinate to Au(I) atom on **1**·$(MeCN)_2$. At last, we can come to the conclusion that the strength of the d(Au) AO interaction is $\sigma(d_{x^2-z^2},d_{y^2}) > \pi(d_{yz}$ or $d_{xz}) > \delta(d_{xy})$.

For the lower energy unfilled orbitals, the combination of 6s and 6p orbitals of Au atoms contributes to the σ, π, σ*, and π* MOs. The $32a_g$ orbital (LUMO) is the admixture of 23% s, 11% p_z, and 5% d_{y^2} components to give the σ bonding orbital. The p_z(Au) AOs combine to form the σ* orbital in $33a_u$. Four π orbitals in $32a_u$, $33a_g$, $34a_u$, and $35a_g$ come from the p_x(Au)−p_x(Au) and p_y(Au)−p_y(Au) interactions, as shown in Table 6. For **1**·$(MeCN)_2$, the $31a_u \rightarrow 32a_g$ excitation configuration with the largest coefficient of 0.67 in the CI wave functions should be responsible for the 507 nm emission. According to the above analyses on the orbital characters of **1**·$(MeCN)_2$ in the excited state, the $31a_u$ orbital (HOMO) has the $\sigma^*(d_{x^2-z^2},d_{y^2})$ characters and the $32a_g$ orbital (LUMO) is the $\sigma(s,p_z)$ bonding orbital. Therefore, the 507 nm emission of **1**·$(MeCN)_2$ is assigned to a $\sigma(s,p_z) \rightarrow \sigma^*(d_{x^2-z^2},d_{y^2})$ transition from the excited state to the ground state, which corresponds to the 490−530 nm emissions of $[Au_2(dcpm)_2]X_2$ (X = Cl^-, ClO_4^-, PF_6^-, and $SO_3CF_3^-$) in acetonitrile at room temperature. It is the increase of electrons in the σ(s) bonding orbitals and the reduction of electrons in the σ*(d) antibonding orbitals in the excited state of **1**·$(MeCN)_2$ that result in the shorter Au−Au distance with respect to in the ground state as shown in Table 3.

Just like those of **1**·$(MeCN)_2$ in the triplet excited state, the frontier molecular orbitals of **2**·$(MeCN)_2$ and **3**·$(MeCN)_2$ have the most Au orbital characters; i.e., the occupied orbitals mainly arise from Au 5d orbitals and the unoccupied orbitals from Au 6s and 6p orbitals (Tables 1 and 2, Supporting Information). But as the thioether ligand is different from the phosphine ligand in the electronic structure, there is some contribution of the remaining lone pair electrons on the sulfur atom to the filled orbitals for **2**·$(MeCN)_2$ and **3**·$(MeCN)_2$. It is worth noting that the relatively lower energy σ(Au−P/S) (18a″) and σ(Au−S) ($21a_u$) bonding orbitals also participate in the emissive transitions for **2**·$(MeCN)_2$ and **3**·$(MeCN)_2$, respectively. In addition, there is some mistake in predicting the order of orbitals in the CIS calculations, because the $26a_g$ as a $\delta(d_{xy})$ bonding orbital is higher in energy than $25a_u$ ($\delta^*(d_{xy})$) for **3**·$(MeCN)_2$, as seen in Supporting Information Table 2. It mainly results from the error of the CIS method. The CIS method for the excited state only corresponds to the HF method for the ground state and only includes some of the electron correlation effects via the mixing of excited determinants. However, we think the CIS method is reliable in the paper, as CIS predicts the majority of orbitals of **1**−**3** in accurate order and energy and comes true the calculations of the relatively large molecules.

$[Au_2(diphosphine)_2]^{2+}$ and $[Pt_2(P_2O_5H_2)_4]^{4-}$ both have vacant coordination sites at the metal atom and display an intense σ-(s/p) → σ*(d) emission with a long lifetime of microseconds in fluid solutions at room temperature. Importantly, the $^3[\sigma^*(d)$-$\sigma(s/p)]$ triplet excited states of both systems have a formal metal−metal single bond and are powerful photoreductants. $[Pt_2(P_2O_5H_2)_4]^{4-}$ is an effective photocatalyst for C−X (X = halide) bond activation via the reactive $[Pt_2\cdots X-C]^*$ intermediate;[90−91,93−95,114] however, the $[Au_2(dppm)_2]^{2+}$ catalyzes the photochemical cleavage of C−X bonds following an electron-transfer mechanism rather than an atom-transfer mechanism.[33,59] $[Au_2(diphosphine)_2]^{2+}$ systems do not react with C−H bonds (including activated ones) photochemically just as $[Pt_2(P_2O_5H_2)_4]^{4-}$ does. Such a discrepancy in the photochemical properties between the gold(I) and platinum(II) systems has been rationalized by Che's studies on $[Au_2(diphosphine)_2]^{2+}$.[31,32] They proposed that the apparent lack of reactivity toward C−H bond activation of the triplet excited states of $[Au_2(diphosphine)_2]^{2+}$ is attributed to the fact that the $^3[\sigma^*(d)\sigma(s)]$ state of the Au(I) complex exists as a solvent/anion exciplex in solution, rendering the gold(I) less accessible toward interacting with the C−H bond by an inner-sphere pathway. In the work, we provide the theoretical evidence for the formation of the adduct of Au(I) complex in the excited state in acetonitrile.

In addition, we also calculated the related platinum(II) complexes $[Pt_2(X)_4(PH_2CH_2PH_2)_2]$ and $[Pt_2(X)_4(PH_2CH_2PH_2)_2]$·$(MeCN)_2$ (X = CN^-, Cl^-, and Br^-) to the famous $[Pt_2(P_2O_5H_2)_4]^{4-}$. The results show the interaction between the Pt(II) and N atoms of $[Pt_2(X)_4(PH_2CH_2PH_2)_2]$·$(MeCN)_2$ is very weak either in the ^1A_g ground state or in the ^3A_u excited state. For example, the $^3[\sigma^*(d)\sigma(p)]$ excited states of $[Pt_2(Cl)_4(PH_2CH_2PH_2)_2]$ and $[Pt_2(Cl)_4(PH_2CH_2PH_2)_2]$·$(MeCN)_2$ give rise to emissions at 420 and 424 nm, respectively. The Pt−N distances of the solvated species are 3.015 Å in the ^1A_g ground state and 5.007 Å in the ^3A_u excited state. The deference between **1**·$(MeCN)_2$ and $[Pt_2(X)_4(PH_2CH_2PH_2)_2]$·$(MeCN)_2$ in the excited-state structure can rationalize why the binuclear platinum(II) complexes can serve as an effective photocatalyst for C−X (X = halide) bond activation via the reactive $[Pt_2\cdots X-C]^*$ but the binuclear Au(I) complexes do not.

3.3. All Possible Geometries and Subtituent Effect of 2 and 2·(MeCN)$_2$. In the calculations, the **2** complex can take chair (Figure 1a, Supporting Information) and boat (Figure 1b, Supporting Information) conformations in the ground state.

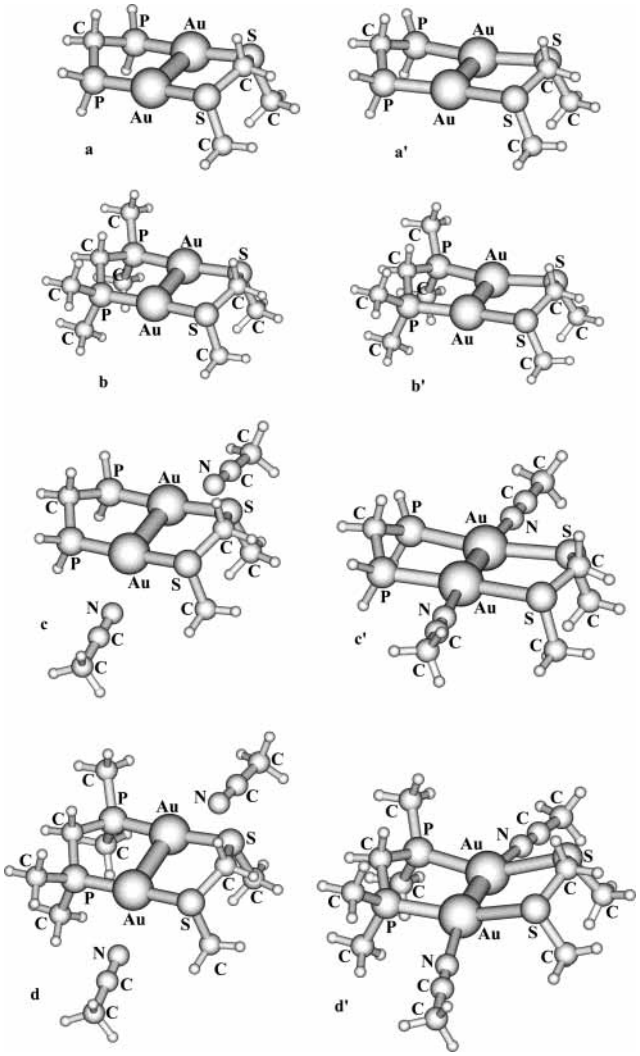

Figure 3. Ground-state (a)−(d) and excited-state (a′)−(d′) structures of $[Au_2(PH_2CH_2PH_2)(SCH_3CH_2SCH_3)]^{2+}$ (**4**), $[Au_2(P(CH_3)_2CH_2P(CH_3)_2)(SCH_3CH_2SCH_3)]^{2+}$ (**5**), $[Au_2(PH_2CH_2PH_2)(SCH_3CH_2SCH_3)]^{2+}\cdot(MeCN)_2$ (**4**·$(MeCN)_2$), and $[Au_2(P(CH_3)_2CH_2P(CH_3)_2)(SCH_3CH_2SCH_3)]^{2+}\cdot(MeCN)_2$ (**5**·$(MeCN)_2$) optimized by the MP2 and CIS methods, respectively.

When **2** adopts the chair configuration and the steric effect is considered, the acetonitrile solvent molecules may contribute to Au(I) atoms from the same side of the $Au_2P_2S_2$ plane or the two sides of the plane to form the weakly solvated **2**·$(MeCN)_2$ moiety, as shown Figure 2a,b (Supporting Information), respectively. The former possesses C_s symmetry and the latter has no symmetry, at the beginning of optimizations on **2**·$(MeCN)_2$. But analysis of optimized geometry parameters indicates the latter also has the C_s symmetry. If the boat conformation is chosen by **2**, the same side contribution like Figure 2c (Supporting Information) is preferred due to the least steric hindrance.

For the excited states of **2** and **2**·$(MeCN)_2$, the CIS method is applied to fully optimize their structures. With respect to each ground state, the lowest energy triplet excited-state geometry is obtained, as shown in Figure 1a′, b′ and Figure 2a′− c′ (Supporting Information). Of particular interest is **2**·$(MeCN)_2$ has an extremely similar excited-state structure except that the C atoms on the eight-membered skeleton adopt trans or cis conformation. Because every conformation for **2** has very similar excited-state properties by analyzing the wave functions, herein only the boat conformation complex in both the gas phase and acetonitrile is discussed in detail.

The calculations on $[Au_2(PH_2CH_2PH_2)(SCH_3CH_2SCH_3)]^{2+}$ (**4**), $[Au_2(P(CH_3)_2CH_2P(CH_3)_2)(SCH_3CH_2SCH_3)]^{2+}$ (**5**), **4**·$(MeCN)_2$, and **5**·$(MeCN)_2$ are carried out to study the substituent effect on the sulfur and/or phosphor atoms of the complexes. The ground- and excited-state structures of **4** and **5** and their solvated species are fully optimized by the MP2 and CIS methods, respectively. The calculated geometry parameters are presented in Tables 2 and 3, and the corresponding structures are depicted in Figure 3. As seen in Tables 2 and 3, the CH_3 substituent on S and/or P atoms in **4** and **5** affects very slightly the molecular geometry. Only the Au−S/P bond length in **4** and **5** is a bit shorter than **2** because the CH_3 substituent enhances the donor ability of the S and P atoms. In the solvated species, the Au−N distance elongates from 2.584 Å of **2**·$(MeCN)_2$ to 2.673 Å of **4**·$(MeCN)_2$ and to 2.774 Å of **5**·$(MeCN)_2$ in the $^1A'$ ground state. The enhancement of the P/S donor ability in **4**·$(MeCN)_2$ and **5**·$(MeCN)_2$ strengthens the P/S → Au bonding, so in the competition among P → Au, S → Au, and N···Au, the N···Au interaction is naturally weakened. Moreover, the steric effect from the CH_3 substituent on the sulfur and/or phosphor atoms is also one reason to elongate the Au−N distance in **4**·$(MeCN)_2$ and **5**·$(MeCN)_2$ with respect to in **2**·$(MeCN)_2$ in the $^1A'$ ground state. A similar case occurs in the $^3A''$ excited states of **2**·$(MeCN)_2$, **4**·$(MeCN)_2$, and **5**·$(MeCN)_2$.

The CIS calculations show that the $^3A''$ excited states of **4** and **5** give rise to the lowest energy phosphorescent emissions at 339 and 337 nm in the gas phase and at 596 and 618 nm in acetonitrile. The analyses on the wave functions indicate that the emissions in both the gas phase and solution originate from the σ(6s) → σ*(5d) (MC) transitions, which are consistent with the 346 nm emission of **2** and the 677 nm emission of **2**·$(MeCN)_2$. Such calculated results reveal that the CH_3 group on the P and S atoms in **4** and **5** as well as **4**·$(MeCN)_2$ and **5**·$(MeCN)_2$ causes the blue shift of emission wavelength with respect to **2** and **2**·$(MeCN)_2$. In **4** and **5**, the stronger donor ability of the P/S atom caused by the CH_3 group increases the Au−P/S σ bonding contribution to the lowest energy emission. As the LUMO and HOMO have σ*(5d) and σ(6s) orbital characters, more Au−P/S σ bonding perturbation to the σ(6s) → σ*(5d) transition should result in larger transition energy and shorter emission wavelength.[54]

3.4. Comparison among Phosphine, Thioether, and Thiolate Complexes in Luminescent Properties. So far, many experiments have studied luminescent properties of phosphine Au(I) thiolate complexes and their excited states have been suggested to be metal to thiolate ligand charge transfer (MLCT) in nature.[20−25] Recently, Bruce and co-workers[20] have reported that a series of binuclear phosphine Au(I) thiolates, $Au_2\{PPh_2(CH_2)_nPPh_2\}\{S(CH_2)_3S\}$ (n = 2−4), display an intense phosphorescent emission in the range of 500−515 nm in the solid state at room temperature, which has been assigned as an Au → S charge transfer (MLCT) transition by experiment and theory.[55]

In the work, a series of binuclear Au(I) complexes with phosphine and/or thioether ligands (**1**−**3**) all produce the lowest energy emission with the MC transition, different from the MLCT transition of the lowest energy emission of Au(I) thiolate complexes. In Figure 4, we display the diagrams of the electron transitions of **1**−**3**, $[Au_2(PH_2CH_2PH_2)(SCH_2S)]$ (**6**),[55] head-to-tail $[Au_2(PH_2CH_2SH)_2]^{2+}$ (**7**),[54] and head-to-head $[Au_2(PH_2CH_2SH)_2]^{2+}$ (**8**),[54] where the comparison between **2** and **6** can provides the most intuitive understanding for the influence of different Au−S bonding characters on the luminescent properties of the Au(I) complexes.

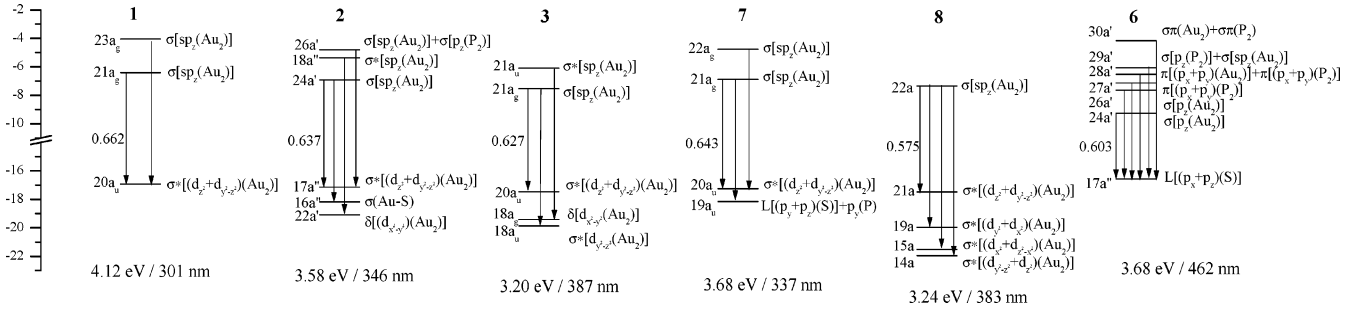

Figure 4. Diagrams of the single electron transitions involved in the CIS wave functions with the |CI coefficient| > 0.1 for the lowest energy emissions of $[Au_2(PH_2CH_2PH_2)_2]^{2+}$ (**1**), $[Au_2(PH_2CH_2PH_2)(SHCH_2SH)]^{2+}$ (**2**), $[Au_2(SHCH_2SH)_2]^{2+}$ (**3**), $[Au_2(PH_2CH_2PH_2)(SCH_2S)]$ (**6**), head-to-tail $[Au_2(PH_2CH_2SH)_2]^{2+}$ (**7**), and head-to-head $[Au_2(PH_2CH_2SH)_2]^{2+}$ (**8**).

We must note that such calculations reported here are carried out considering only the cations for **1**−**3**, **7**, and **8** without the inclusion of the crystal environment. This approximation is reasonable for the purpose of the present study because the crystal field is crucial for getting reasonable orbital energies, but the crystal environment does not necessarily modify either the ordering or the relative orbital energies of the complex. Therefore, the relative energies of the different states reported here should not be altered if isotropic fields are included. For systems that present short contacts between cation and counteranion, some of the conclusions reported here may not be able to be applied directly. Thus, to conveniently compare the transitions of cations **1**−**3**, **7**, and **8** with neutral **6**, we shift all the orbital levels of **6** to the region of such cations; namely, the energy of each orbital of **6** subtracts 10 eV.

Figure 4 shows that the HOMO → LUMO excitation configuration of the Au(I) complexes has the largest coefficient in CI wave functions, which is responsible for the emissive energy and transition property. Apparently, **1**−**3**, **7**, and **8** have very similar orbital characters because the HOMO is the σ^*-[d(Au_2)] character mainly arising from the combination of d_{z^2}(Au) and $d_{y^2-z^2}$(Au) orbitals and LUMO is composed of σ-[$sp_z(Au_2)$] orbitals. (The *z* axis goes through the two Au(I) atoms for these Au(I) complexes; the Au and P atoms of **1** lie upon the *xz* plane and the Au and P/S atoms lie upon the *yz* plane for the other complexes.) However, the HOMO of **6** is the lone pair electrons of the S atom and LUMO comes from σ[$p_z(Au_2)$] orbitals. Therefore, the emissions of **1**−**3**, **7**, and **8** are the MC transitions in nature whereas the emission of **6** is attributable to MLCT transition. For **2** and **6**, the only difference is the bonding characters between the Au and S atoms, which results in the difference of the transition properties, emissive energy, and excited-state geometry. The lowest energy $^3A''$ excited state of **6** presents the Au−Au distance of 2.879 Å, shorter than 3.011 Å in the $^1A'$ ground state, as seen in Table 3 of the Supporting Information.[55] Moreover, the bite distance of S···S shortens from 3.200 Å in the ground state to 2.890 Å in the excited state. As shown in Table 2, the Au−Au distance of **2** reduces from 2.989 Å in the $^3A''$ excited state to 2.708 Å in the $^1A'$ ground state, but the S···S bite distance changes slightly (0.05 Å). It is not difficult to see that the approach of the S atoms in the excited state of **6** strongly destabilizes the orbital with S lone pair electron character, which makes the L(S) constitute the HOMO unlike the σ^*[d(Au_2)] HOMO of **2**. Certainly, the interaction of L(S) is dominant in reducing the emissive energy of **6** (2.68 eV, 462 nm) relative to **2** (3.58 eV, 346 nm) as both LUMOs are the Au−Au bonding orbitals and the stabilized energy of the LUMOs from Au−Au interaction is approximately equal.

With respect to **1**−**3**, **7**, and **8** cations that produce emissions with the MC transitions, the comparison of orbital energy is meaningful. The H−L energy gap (eV) is 10.52 (**1**) > 10.37 (**7**) > 10.21 (**2**) > 10.14 (**8**) > 9.94 (**3**), which parallels with the emissive energy of 4.12 (**1**) > 3.68 (**7**) > 3.58 (**2**) > 3.24 (**8**) > 3.20 (**3**). **2**, **7**, and **8** as isomers should possess the close emissive energy due to the similar frontier orbital characters, but **8** is about 0.4 eV (40 nm) lower in the emissive energy than **2** and **7**. This may result from the instability of the isomer **8** structure.

TABLE 7: Optimized Geometry Parameters of the Lowest Energy Triplet Excited State by the UMP2 Method for Complexes $[Au_2(PH_2CH_2PH_2)_2]^{2+}$ (1), $[Au_2(PH_2CH_2PH_2)(SHCH_2SH)]^{2+}$ (2), $[Au_2(SHCH_2SH)_2]^{2+}$ (3), Head-to-Tail $[Au_2(PH_2CH_2SH)_2]^{2+}$ (7), and Head-to-Head $[Au_2(PH_2CH_2SH)_2]^{2+}$ (8), Together with the Calculated Transition Energy between the Excited State and the Corresponding Ground State

parameters[a]	**1** ^3A_u	**2** $^3A''$	**3** ^3A_u	**7** ^3A_u	**8** ^3A
Au−Au	2.678	2.620	2.583	2.619	2.572
Au−P	2.404	2.399		2.402	2.379
Au−S		2.491	2.500	2.491	2.578
P−C	1.877	1.878		1.883	1.882
S−C		1.871	1.871	1.871	1.857
P···P	3.109	3.133			
S···S		3.273	3.275		
P···S				3.204	3.167
P−Au−S		166.3		165.9	
P−Au−P	169.7				175.0
S−Au−S			164.1		159.0
P−Au−Au	95.1	96.1		93.0	92.5
S−Au−Au		97.5	98.0	100.5	100.5
P/S−Au−Au−S/P	180.0	−178.7	180.0	−176.6	−172.5
ΔE_{UMP2} (eV/nm)[b]	3.57/347	3.26/380	2.84/437	3.34/371	3.01/412
ΔE_{CIS} (eV/nm)[c]	4.12/301	3.58/346	3.20/387	3.68/337	3.24/383

[a] Distances in angstroms, and bond angles and dihedral angles in degrees. [b] The emissive energy (eV/nm) from the UMP2 calculations. [c] The emissive energy (eV/nm) from the CIS calculations.

3.5. UMP2 Calculations. In this paper, we use the unrestricted MP2 method to optimize the lowest energy triplet excited state of **1**−**3**, **7**, and **8**, to certify the validity of such CIS calculations on one hand and to shed some light into the Au−Au bonding properties of the excited state on the other hand. The optimized main geometry parameters related to the triplet excited state are given in Table 7. Compared with the CIS optimized geometry of **1**−**3**, **7**, and **8** as shown in Table 2 and Table 3 (Supporting Information),[54] the UMP2 optimized geometries are more unrelaxed, especially for the Au(I)−Au(I) and Au−P/S bonds. This is because more electron correlation effects are included in the UMP2 method than in the CIS method. Except for **8**, the Au(I)−Au(I), Au−P, and Au−S bond lengths in the UMP2 calculations are about 0.10, 0.14, and 0.21 Å shorter than corresponding ones in the CIS calculations. The Au(I)−Au(I) distance of **8** optimized by the UMP2 method shortens about 0.42 Å relative to the CIS optimized one. A

TABLE 8: Calculated Au−Au Stretching Frequencies for the Ground States and Lowest Energy Triplet Excited States of Complexes $[Au_2(PH_2CH_2PH_2)_2]^{2+}$ (1), $[Au_2(PH_2CH_2PH_2)(SHCH_2SH)]^{2+}$ (2), $[Au_2(SHCH_2SH)_2]^{2+}$ (3), $[Au_2(PH_2CH_2PH_2)(CH_3SCH_2SCH_3)]^{2+}$ (4), $[Au_2(P(CH_3)_2CH_2P(CH_3)_2)(CH_3SCH_2SCH_3)]^{2+}$ (5), Head-to-Tail $[Au_2(PH_2CH_2SH)_2]^{2+}$ (7), and Head-to-Head $[Au_2(PH_2CH_2SH)_2]^{2+}$ (8)

		1	2	3	7	8
ground state	freq (cm^{-1})	89	96	101	96	97
	Au−Au (Å)	3.033	2.989	2.944	2.979	2.972
triplet excited state	freq (cm^{-1})	144	164	179	165	189
	Au−Au (Å)	2.678	2.620	2.583	2.619	2.572

possible reason is that the MP2 method overestimates the bonding Au(I)−Au(I) interaction (2.572 Å), as seen in Table 7, whereas the CIS method underestimates the diffuse Au(I)−Au(I) interaction (2.994 Å), as seen in Table 3 (Supporting Information).[41−44,115] But as the HOMO and LUMO characters described by the two methods are identical, the difference in the geometry structure is acceptable here.

In Table 7, we also summarize the emissive energy for **1**−**3**, **7**, and **8** under the UMP2 and CIS calculations. The emissive energy of the UMP2 calculations is a bit lower than the CIS results, which is consistent with the CIS method overestimating the transition energy.[72,82−84] For **1**, the emissive energy is calculated at 3.57 eV (347 nm) and 4.12 eV (301 nm) at the UMP2 and CIS levels, respectively. Apparently, the result predicted by the UMP2 method is closer to the experimental 3.44 eV (360 nm) emission for $[Au_2(dcpm)_2]^{2+}$ in the solid state.[31,32] Because in the UMP2 and CIS calculations the difference of the emissive energy is very small, 0.23−0.55 eV (34−46 nm), the characters of HOMO and LUMO are identical, and the geometry structure is approximately parallel, we think the CIS results are reliable for the Au(I) systems in the paper.

We have carried out frequency calculations on **1**−**3**, **7**, and **8** at the MP2 level for the ground state and the triplet excited state. No imaginary frequencies available indicate that the ground- and excited-state geometry structures of such Au(I) complexes are minimum points. The calculated Au−Au stretching frequencies (Table 8) fall well within the range of the experiment[30,101,116−118] and calculations.[56,102,115] The 89−101 cm^{-1} Au−Au stretching frequency of the ground state agrees well with the experimental 88 cm^{-1} for $[Au_2(dcpm)_2]\cdot(ClO_4)_2$,[55] 71 cm^{-1} for $[Au_2(dmpm)_2]\cdot Cl_2$,[116] and 69 cm^{-1} for $[Au_2(dmpm)_2]\cdot(PF_6)_2$,[116] whereas the 144−189 cm^{-1} frequency of the excited state corresponds to experimental Au(II)−Au(II), 157 cm^{-1} for $[Au_2Cl_2(CH_2PPh_2S)_2]$[101] and 162 cm^{-1} for $[Au_2Cl_2(CH_2PPh_2CH_2)_2]$.[101,118] The frequency calculations suggest that the Au(I)−Au(I) interaction is weak in the ground state (mean 2.98 Å Au−Au distance and 95 cm^{-1} Au−Au stretching frequency) but is strongly enhanced in the excited state (mean 2.60 Å Au−Au distance and 160 cm^{-1} Au−Au stretching frequency). Table 8 shows the Au−Au stretching frequency is correlated with the Au−Au distance, namely, stronger frequency, shorter distance.

4. Conclusion

The ab initio studies on the spectroscopic properties of **1**−**3** as well as their solvated species show the $^3[\sigma^*(d)\sigma(s)]$ excited states give the emissions at 300−390 nm in the gas phase and at 500−730 nm in acetonitrile. The coordination of acetonitrile to the gold atom in the $^3[\sigma^*(d)\sigma(s)]$ excited state is responsible for such a large red shift. The comparison of $\mathbf{1}\cdot(MeCN)_2$ and $[Pt_2(X)_4(PH_2CH_2PH_2)_2]\cdot(MeCN)_2$ (X = CN^-, Cl^-, and Br^-) in the excited-state geometry rationalizes the difference between the binuclear gold(I) and platinum(II) phosphine complexes in catalyzing the C−X bonds.

For **2**, the possible geometries are optimized in the gas phase and solution, which all have very similar geometry structures of the excited state and luminescent properties. The substituent effect of methyl groups on P and/or S atoms for **2** and $\mathbf{2}\cdot(MeCN)_2$ only affects the transition energy of the lowest energy emission but does not change the MC transition in nature, showing the rationality of the approximation of the hydrogen in place of the heavy subtituent on the P/S atoms. The comparison between **2** (thioether) and **6** (thiolate) suggests that the different bonding characters between the Au(I) and S atoms result in the lowest energy emission with the MC and MLCT transition properties, respectively.

Finally, the UMP2 calculations on **1**−**3**, **7**, and **8** confirm the CIS results in both optimized geometry and emissive energy of the $^3[\sigma^*(d)\sigma(s)]$ state.[54] The CIS method is safe for the studies in the paper. We also hope that our studies can provide some theoretical support for the experimental observations, especially for the existing and/or potential applications of Au(I) complexes.[1,2,24,29−34,119−125]

Acknowledgment. This work is supported by the Natural Science Foundation of China (20173021).

Supporting Information Available: Tables of molecular orbital contributions and geometry parameters and images of the optimized ground-state structures. This material is available free of charge via the Internet at http://pubs.acs.org.

References and Notes

(1) Lee, Y. A.; McGarrah, J. E.; Lachicotte, R. J.; Eisenberg, R. *J. Am. Chem. Soc.* **2002**, *124*, 10662.

(2) Mansour, M. A.; Connick, W. B.; Lachicotte, R. J.; Gysling, H. J.; Eisenberg, R. *J. Am. Chem. Soc.* **1998**, *120*, 1329.

(3) Bryce, A. B.; Charnochk, J. M.; Pattrichk, R. A. D.; Lennie, A. R. *J. Phys. Chem. A* **2003**, *107*, 2516.

(4) White-Morris, R. L.; Olmstead, M. M.; Balch, A. L. *J. Am. Chem. Soc.* **2003**, *125*, 1033.

(5) White-Morris, R. L.; Olmstead, M. M.; Jiang, F.; Tinti, D. S.; Balch, A. L. *J. Am. Chem. Soc.* **2002**, *124*, 2327.

(6) Vickery, J. C.; Lomstead, M. M.; Fung, E. Y.; Balch, A. L. *Angew. Chem., Int. Ed. Engl.* **1997**, *36*, 1179.

(7) Salama, T. M.; Shido, T.; Ohnishi, R.; Ichikawa, M. *J. Phys. Chem.* **1996**, *100*, 3688.

(8) Gimeno, M C.; Laguna, A. *Chem. Rev.* **1997**, *97*, 511.

(9) Fernández, E. J.; López-de-Luzuriaga, J. M.; Monge, M.; Rodríguez, M. A.; Crespo, O.; Gimeno, M. C.; Laguna, A.; Jones, P. G. *Chem. Eur. J.* **2000**, *6*, 636.

(10) Bardají, M.; Laguna, A.; Pérez, M. R. *Organometallics* **2002**, *21*, 1877.

(11) Codina, A.; Fernández, E. J.; Jones, P. G.; Laguna, A.; López-de-Luzuriaga, J. M.; Monge, M.; Olmos, M. E.; Pérez, J.; Rodríguez, M. A. *J. Am. Chem. Soc.* **2002**, *124*, 6781.

(12) Alloway, D. M.; Hofmann, M.; Smith, D. L.; Gruhn, N. E.; Graham, A. L.; Colorado, R., Jr.; Wysocki, V. H.; Lee, T. R.; Lee, P. A.; Armstrong, N. R. *J. Phys. Chem. B* **2003**, *107*, 11690.

(13) Forward, J. M.; Assefa, Z.; Facker, J. P., Jr. *J. Am. Chem. Soc.* **1995**, *117*, 9103.

(14) Dávila, R. M.; Elduque, A.; Grant, T.; Staples, R. J.; Fackler, J. P., Jr. *Inorg. Chem.* **1993**, *32*, 1749.

(15) King, C.; Khan, M. N. I.; Staples, R. J.; Fackler, J. P., Jr. *Inorg. Chem.* **1992**, *31*, 3236.

(16) Lu, W.; Xiang, H.-F.; Zhu, N.; Che, C.-M. *Organometallics* **2002**, *21*, 2343.

(17) Che, C.-M.; Chao, H.-Y.; Miskowski, V. M.; Li, Y.; Cheung, K.-K. *J. Am. Chem. Soc.* **2001**, *123*, 4985.

(18) Lu, W.; Zhu, N.; Che, C.-M. *J. Organomet. Chem.* **2003**, *670*, 11.

(19) Schwerdtfeger, P.; Bruce, A. E.; Bruce, M. R. M. *J. Am. Chem. Soc.* **1998**, *120*, 6587.

(20) Jones, W. B.; Yuan, J.; Narayanaswamy, R.; Young, M. A.; Elder, R. C.; Bruce, A. E.; Bruce, M. R. M. *Inorg. Chem.* **1995**, *34*, 1996.

(21) Narayanaswamy, R.; Young, M. A.; Parkhurst, E.; Ouellette, M.; Kerr, M. E.; Ho, K. M.; Elder, R. C.; Bruce, A. E.; Bruce, M. R. M. *Inorg. Chem.* **1993**, *32*, 2506.
(22) Hanna, S. D.; Zink, J. I. *Inorg. Chem.* **1996**, *35*, 297.
(23) Hanna, S. D.; Khan, S. I.; Zink, J. I. *Inorg. Chem.* **1996**, *35*, 5813.
(24) Yam, V.-W. W.; Lo, K. K. W. *Chem. Soc. Rev.* **1999**, *28*, 323.
(25) Yam, V. W.-W.; Cheng, E. C.-C.; Zhou, Z.-Y. *Angew. Chem., Int. Ed.* **2000**, *39*, 1683.
(26) Yam, V. W.-W.; Chan, C.-L.; Li, C.-K.; Wong, K. M.-C. *Coord. Chem. Rev.* **2001**, *216*−*217*, 173.
(27) Yam, V. W.-W.; Chan, C.-L.; Choi, S. W.-K.; Wong, K. M.-C.; Cheng, E. C.-C.; Yu, S.-C.; Ng, P.-K.; Chan, W.-K.; Cheung, K.-K. *Chem. Commun.* **2000**, 53.
(28) Watase, S.; Nakamoto, M.; Kitamura, T.; Kanehisa, N.; Kai, Y. *J. Chem. Soc., Dalton Trans.* **2000**, 3585.
(29) King, C.; Wang, J. C.; Khan, M. N. I.; Fackler, J. P., Jr. *Inorg. Chem.* **1989**, *28*, 2145.
(30) Leung, K. H.; Phillips, D. L.; Tse, M.-C.; Che, C.-M.; Miskowski, V. M. *J. Am. Chem. Soc.* **1999**, *121*, 4799.
(31) Fu, W.-F.; Chan, K.-C.; Miskowski, V. M.; Che, C.-M. *Angew. Chem., Int. Ed. Engl.* **1999**, *38*, 2783.
(32) Fu, W.-F.; Chan, K.-C.; Cheung, K.-K.; Che, C.-M. *Chem. Eur. J.* **2001**, *7*, 4656.
(33) Che, C.-M.; Kwong, H.-L.; Yam, V. W.-W.; Cho, K.-C. *J. Chem. Soc., Chem. Commun.* **1989**, 885.
(34) Che, C.-M.; Kwong, H.-L.; Poon, C.-K. *J. Chem. Soc., Dalton Trans.* **1990**, 3215.
(35) Jones, P. G. *Gold Bull.* **1986**, *19*, 46−54; **1983**, *16*, 114−120; **1981**, *14*, 159−168; **1981**, *14*, 102.
(36) Pathaneni, S. S.; Desiraju, G. R. *J. Chem. Soc., Dalton Trans.* **1993**, 319.
(37) Schmidbaur, H.; Graf, W.; Müller, G. *Angew. Chem., Int. Ed. Engl.* **1988**, *27*, 417.
(38) Harwell, D. E.; Mortimer, M. D.; Knobler, C. B.; Anet, F. A. L.; Hawthorne, M. F. *J. Am. Chem. Soc.* **1996**, *118*, 2679.
(39) Balch, A. L.; Fung, E. Y.; Olmstead, M. M. *J. Am. Chem. Soc.* **1990**, *112*, 5181.
(40) Tang, S. S.; Chang, C.-P.; Lin, I. J. B.; Liou, L.-S.; Wang, J.-C. *Inorg. Chem.* **1997**, *36*, 2294.
(41) Pyykkö, P.; Runeberg, N.; Mendizabal, F. *Chem. Eur. J.* **1997**, *3*, 1451.
(42) Pyykkö, P.; Mendizabal, F. *Chem. Eur. J.* **1997**, *3*, 1458.
(43) Pyykkö, P.; Mendizabal, F. *Inorg. Chem.* **1998**, *37*, 3018.
(44) Pyykkö, P. *Chem. Rev.* **1997**, *97*, 597.
(45) Pyykkö, P. *Chem. Rev.* **1988**, *88*, 563.
(46) Pyykkö, P.; Schneider, W.; Bauer, A.; Bayler, A.; Schmidbaur, H. *Chem. Commun.* **1997**, 1111.
(47) Pyykkö, P.; Zhao, Y.-F. *Angew. Chem., Int. Ed. Engl.* **1991**, *30*, 604; *Angew. Chem.* **1991**, *103*, 622.
(48) Li, J.; Pyykkö, P. *Chem. Phys. Lett.* **1992**, *197*, 586.
(49) Pyykkö, P.; Li, J.; Runeberg, N. *Chem. Phys. Lett.* **1994**, *218*, 133.
(50) Li, J.; Pyykkö, P. *Inorg. Chem.* **1993**, *32*, 2630.
(51) Pyykkö, P. *Science* **2000**, *290*, 64.
(52) Zank, J.; Schier, A.; Schmidbaur, H. *J. Chem. Soc., Dalton Trans.* **1998**, 323.
(53) Zhang, H.-X.; Che, C.-M. *Chem. Eur. J.* **2001**, *7*, 4887.
(54) Pan, Q.-J.; Zhang, H.-X. *Inorg. Chem.* **2004**, *43*, 593.
(55) Pan, Q.-J.; Zhang, H.-X. *J. Chem. Phys.* **2003**, *119*, 4346.
(56) Pan, Q.-J.; Zhang, H.-X. *Eur. J. Inorg. Chem.* **2003**, 4202.
(57) Kim, C. D.; Pillet, S.; Wu, G.; Fullagar, W. K.; Coppens, P. *Acta Crystallogr.* **2002**, *A58*, 133.
(58) Novozhilova, I. V.; Volkov, A. V.; Coppens, P. *J. Am. Chem. Soc.* **2003**, *125*, 1079.
(59) Li, D.; Che, C.-M.; Kwong, H.-L.; Yam, V. W.-W. *J. Chem. Soc., Dalton Trans.* **1992**, 3325.
(60) Schaefer, W. P.; Marsh, R. E.; McCleskey, T. M.; Gray, H. B. *Acta Crystallogr.* **1991**, *C47*, 2553.
(61) Porter, L. C.; Khan, Md. N. I.; King, C.; Fackler, J. P., Jr. *Acta Crystallogr.* **1989**, *C45*, 947.
(62) Wang, J.-C.; Khan, Md. N. I.; Fackler, J. P., Jr. *Acta Crystallogr.* **1989**, *C45*, 1482.
(63) Kozelka, J.; Oswald, H. R.; Dubler, E. *Acta Crystallogr.* **1986**, *C42*, 1007.
(64) Briant, C. E.; Hall, K. P.; Mingos, D. M. P. *J. Organomet. Chem.* **1982**, *229*, C5.
(65) Shain, J.; Fackler, J. P., Jr. *Inorg. Chim. Acta* **1987**, *131*, 157.
(66) Payne, N. C.; Puddephatt, R. J.; Ravindranath, R.; Treurnicht, I. *Can. J. Chem.* **1988**, *66*, 3176.
(67) Bardají, M.; Jones, P. G.; Laguna, A.; Villacampa, M. D.; Villaverde, N. *J. Chem. Soc., Dalton Trans.* **2003**, 4529.
(68) Fernández, E. J.; López-de-Luzuraga, J. M.; Monge, M.; Rodríguez, M. A.; Crespo, O.; Gimeno, M. C.; Laguna, A.; Jones, P. G. *Inorg. Chem.* **1998**, *37*, 6002.
(69) Frenking, G.; Fröhlich, N. *Chem. Rev.* **2000**, *100*, 717.
(70) van Zyl, W. E.; López-de-Luzuriaga, J. M.; Mohamed, A. A.; Staples, R. J.; Fackler, J. P., Jr. *Inorg. Chem.* **2002**, *41*, 4579.
(71) van Zyl, W. E.; López-de-Luzuriaga, J. M.; Fackler, J. P., Jr. *J. Mol. Struct.* **2000**, *516*, 99.
(72) Khan, Md. N. I.; Fackler, J. P., Jr.; King, C.; Wang, J. C.; Wang, S. *Inorg. Chem.* **1988**, *27*, 1672.
(73) Foresman, J. B.; Head-Gordon, M.; Pople, J. A.; Frisch, M. J. *J. Phys. Chem.* **1992**, *96*, 135.
(74) Raghavachari, K.; Pople, J. A. *Int. J. Quantum Chem.* **1981**, *20*, 1067.
(75) Frisch, M. J.; Trucks, G. W.; Schlegel, H. B.; Scuseria, G. E.; Robb, M. A.; Cheeseman, J. R.; Zakrzewski, V. G.; Montgomery, J. A., Jr.; Stratmann, R. E.; Burant, J. C.; Dapprich, S.; Millam, J. M.; Daniels, A. D.; Kudin, K. N.; Strain, M. C.; Farkas, O.; Tomasi, J.; Barone, V.; Cossi, M.; Cammi, R.; Mennucci, B.; Pomelli, C.; Adamo, C.; Clifford, S.; Ochterski, J.; Petersson, G. A.; Ayala, P. Y.; Cui, Q.; Morokuma, K.; Malick, D. K.; Rabuck, A. D.; Raghavachari, K.; Foresman, J. B.; Cioslowski, J.; Ortiz, J. V.; Baboul, A. G.; Stefanov, B. B.; Liu, G.; Liashenko, A.; Piskorz, P.; Komaromi, I.; Gomperts, R.; Martin, R. L.; Fox, D. J.; Keith, T.; Al-Laham, M. A.; Peng, C. Y.; Nanayakkara, A.; Challacombe, M.; Gill, P. M. W.; Johnson, B.; Chen, W.; Wong, M. W.; Andres, J. L.; Gonzalez, C.; Head-Gordon, M.; Replogle, E. S.; Pople, J. A. *Gaussian 98*, Revision A.9; Gaussian, Inc., Pittsburgh, PA, 1998.
(76) Møller, C.; Plesset, M. S. *Phys. Rev.* **1934**, *46*, 618.
(77) Fernández, E. J.; Gimeno, M. C.; Jones, P. G.; Laguna, A.; Laguna, M.; López-de-Luzuriaga, J. M.; Rodriguez, M. A. *Chem. Ber.* **1995**, *128*, 121.
(78) Bayse, C. A. *J. Phys. Chem. A* **2001**, *105*, 5902.
(79) Naito, K.; Sakurai, M.; Egusa, S. *J. Phys. Chem. A* **1997**, *101*, 2350.
(80) Bowmaker, B. A.; Schmidbaur, H.; Krüger, S.; Rösch, N. *Inorg. Chem.* **1997**, *36*, 1754.
(81) Häberlen, O. D.; Rösch, N. *J. Phys. Chem.* **1993**, *97*, 4970.
(82) Foresman, J. B.; Frisch, Æ. *Exploring Chemistry with Electronic Structure Methods*, 2nd ed.; Gaussian, Inc.: Pittsburgh, PA, 1996.
(83) Halls, M. D.; Schlegel, H. B. *Chem. Mater.* **2001**, *13*, 2632.
(84) Casida, M. E.; Jamorski, C.; Casida, K. C.; Salahub, D. R. *J. Chem. Phys.* **1998**, *108*, 4439.
(85) Wadt, W. R.; Hay, P. J. *J. Chem. Phys.* **1985**, *82*, 284.
(86) Hay, P. J.; Wadt, W. R. *J. Chem. Phys.* **1985**, *82*, 299.
(87) Chan, W.-H.; Mak, T. C. W.; Che, C.-M. *J. Chem. Soc., Dalton Trans.* **1998**, 2275.
(88) Kunkely, H.; Vogler, A. *J. Am. Chem. Soc.* **1990**, *112*, 5625.
(89) Pettijohn, C. N.; Jochnowitz, E. B.; Chuong, B.; Nagle, J. K.; Vogler, A. *Coord. Chem. Rev.* **1998**, *171*, 85.
(90) Sweeney, R. J.; Harvey, E. L.; Gray, H. B. *Coord. Chem. Rev.* **1990**, *105*, 23.
(91) Smith, D. C.; Gray, H. B. *Coord. Chem. Rev.* **1990**, *100*, 169.
(92) Rice, S. F.; Gray, H. B. *J. Am. Chem. Soc.* **1983**, *105*, 4571.
(93) Roundhill, D. M.; Gray, H. B.; Che, C.-M. *Acc. Chem. Res.* **1989**, *22*, 55.
(94) Che, C.-M.; Lee, W.-M.; Cho, K.-C.; Harvey, P. D.; Gray, H. B. *J. Phys. Chem.* **1989**, *93*, 3095.
(95) Zipp, A. P. *Coord. Chem. Rev.* **1988**, *84*, 47.
(96) Thiel, D. J.; Livins, P.; Stern, E. A.; Lewis, A. *Nature* **1993**, *362*, 40.
(97) Peterson, J. R.; Kalyanasundaram, K. *J. Phys. Chem.* **1985**, *89*, 2486.
(98) Roundhill, D. M.; Shen, Z.-P.; King, C.; Atherton, S. J. *J. Phys. Chem.* **1988**, *92*, 4088.
(99) Bondi, A. *J. Phys. Chem.* **1964**, *68*, 441.
(100) Basil, J. D.; Murray, H. H.; Fackler, J. P., Jr.; Tocher, J.; Mazany, A. M.; Trzcinska-Bancroft, B.; Knachel, H.; Dudis, D.; Delord, T. J.; Marler, D. O. *J. Am. Chem. Soc.* **1985**, *107*, 6908.
(101) Carlson, T. F.; Fackler, J. P., Jr. *J. Organomet. Chem.* **2000**, *596*, 237.
(102) Barysz, M.; Pyykkö, P. *Chem. Phys. Lett.* **2000**, *325*, 225.
(103) Trzcinska-Bancroft, B.; Khan, Md. N. I.; Fackler, J. P., Jr. *Organometallics* **1988**, *7*, 993.
(104) Mazany, A. M.; Fackler, J. P., Jr. *J. Am. Chem. Soc.* **1984**, *106*, 801.
(105) Seidel, S.; Seppelt, K. *Science* **2000**, *290*, 117.
(106) Ganapathy, S.; Fournier, M.; Paul, J. F.; Delevoye, L.; Guelton, M.; Amoureux, J. P. *J. Am. Chem. Soc.* **2002**, *124*, 7821.
(107) Duclusaud, H.; Borshch, S. A. *Inorg. Chem.* **1999**, *38*, 3489.
(108) Jansen, S. A.; Singh, D. J.; Wang, S.-H. *Chem. Mater.* **1994**, *6*, 146.
(109) Suaud, N.; Gaita-Ariño, A.; Clemente-Juan, J. M.; Sánchez-Marin, J.; Coronado, E. *J. Am. Chem. Soc.* **2002**, *124*, 15134.
(110) Reed, A. E.; Weinstock, R. B.; Weinhold, F. *J. Chem. Phys.* **1985**, *83*, 735.

(111) Foster, J. P.; Weinhold, F. *J. Am. Chem. Soc.* **1980**, *102*, 7211.
(112) Reed, A. E.; Curtiss, L. A.; Weinhold, F. *Chem. Rev.* **1988**, *88*, 899.
(113) Löwdin, R.-D. *Phys. Rev.* **1955**, *97*, 1474.
(114) Roundhill, D. M. *J. Am. Chem. Soc.* **1985**, *107*, 4354.
(115) Rawashdeh-Omary, M. A.; Omary, M. A.; Patterson, H. H.; Fackler, J. P., Jr. *J. Am. Chem. Soc.* **2001**, *123*, 11237.
(116) Perreault, D.; Drouin, M.; Michel, A.; Miskowski, V. M.; Schaefer, W. P.; Harvey, P. D. *Inorg. Chem.* **1992**, *31*, 695.
(117) Farrell, F. J.; Spiro, T. G. *Inorg. Chem.* **1971**, *10*, 1606.
(118) Clark, R. J. H.; Tocher, J. H.; Fackler, J. P., Jr.; Neira, R.; Murray, H. H.; Knachel, H. J. *J. Organomet. Chem.* **1986**, *303*, 437.
(119) McKeage, M. J.; Maharaj, L.; Berners-Price, S. J. *Coord. Chem. Rev.* **2002**, *232*, 127.
(120) Berners-Price, S. J.; Bowen, R. J.; Galettis, P.; Healy, P. C.; McKeage, M. J. *Coord. Chem. Rev.* **1999**, *185*−*186*, 823.
(121) Navarro, M.; Pérez, H.; Sánchez-Delgado, R. A. *J. Med. Chem.* **1997**, *40*, 1937.
(122) Berners-Price, S. J.; Girard, G. R.; Hill, D. T.; Sutton, B. M.; Jarrett, P. S.; Faucette, L. F.; Johnson, R. K.; Mirabelli, C. K.; Sadler, P. J. *J. Med. Chem.* **1990**, *33*, 1386.
(123) Corey, E. J.; Mahrotra, M. M.; Khan, A. U. *Science* **1987**, *236*, 68.
(124) Mirabelli, C. K.; Johnson, R. K.; Hill, D. T.; Faucette, L. F.; Girard, G. R.; Kuo, G. Y.; Sung, C. M.; Crooke, S. T. *J. Med. Chem.* **1986**, *29*, 218.
(125) Weinstock, J.; Sutton, B. M.; Kuo, G. Y.; Walz, D. T.; Dimartino, M. J. *J. Med. Chem.* **1974**, *17*, 139.